RIPs Interact with OsFH5 and Control the Rice Morphology by Affecting Stability of OsFH5

Shuwei Chang
Shanghai Jiao Tong University
Litao Yang
Shanghai Jiao Tong University
Wanqi Liang
Shanghai Jiao Tong University
Qi Xie
Institute of Genetics and Developmental Biology Chinese Academy of Sciences
Guoqiang Huang
Shanghai Jiao Tong University
Duoxiang Wang
Shanghai Jiao Tong University
Wanwan Zhu
Shanghai Jiao Tong University
Dabing Zhang (zhangdb@sjtu.edu.cn)
Shanghai Jiao Tong University https://orcid.org/0000-0002-1764-2929

Original article

Keywords: SIAH, oligomers, OsFH5, dwarf, angles, roots, morphology

Posted Date: July 14th, 2021

DOI: https://doi.org/10.21203/rs.3.rs-666132/v1

Abstract

E3 ubiquitin ligases have been more widely reported to mediate the degradation of target proteins. In our research, one SIAH type E3 ligase was identified, named RIP1, and there are five genes were found to be highly homologous to it, named RIP2 to RIP6 dividedly. Y2H and BiFC were carried out to prove the interaction between RIPs and OsFH5, moreover, homo- and hetero- oligomers can be formed among RIPs and they all can affect the localization of OsFH5. Degradation experiments showed that RIP1 is able to slow down the degradation rate of OsFH5, and also RIP5, RIP6. There was no obvious phenotype in both RIP1 overexpression and mutant transgenic lines, whereas in *rips* multi-knock out lines showed up similar defects to *osfh5*, such as, dwarf height; less smooth and rounder seeds; leaves width became wilder. Otherwise, *rips* also exhibit some special phenotypes, for instance, the angles between leaves and stems were appreciable enlarged; spiral crimped roots. In addition, microfilaments organization in *rips* appeared disordered than wild type. All above illustrate that RIPs influence morphology by interacting with OsFH5 and affecting its subcellular localization, stability or maybe involved in other pathways in rice.

Introduction

E3 ubiquitin ligases are the most abundant proteins in quantity in eukaryote (Mazzucotelli et al, 2006b, Liyuan et al, 2013, Michael et al, 2015), E3s catalyze the covalent attachment of ubiquitin to substrates with the help of E1 (ubiquitin-activating enzyme) and E2 (ubiquitin-conjugating enzyme) (Buetow and Huang, 2016). It is well know that the critical function of E3s are mediating degradation of substrates (Mazzucotelli et al, 2006a), but different kinds of ubiquitination, including mono-ubiquitination, poly-ubiquitination or ubiquitin chains formed by different lysine of ubiquitin will produce different outcomes (Buetow and Huang, 2016, French et al, 2021, Swatek and Komander, 2016), including directing substrates into endocytic pathway; regulating kinase activation; monoubiquitylation participate in DNA repair; chromatin remodeling and other cellular signals (Nakazawa et al, 2020). In addition, ubiquitin can also be acetylated on Lys, or phosphorylated on Ser, Thr or Tyr residues, and every kind of modification has the potential to alter the signaling outcomes (Swatek and Komander, 2016). Moreover, ubiquitin-like molecules modifications, such as, SUMO (small ubiquitin-like modifier), NEDD (Neural precursor cell-Expressed Developmentally down-regulated) or ATG (autophagy-related gene) 8, also add significant complexity to the system (Miura and Hasegawa, 2010, Ghimire et al, 2020, Mergner and Schwechheimer, 2014, Bu et al, 2020). Last, modifications of E3 ligases also affect theirs' activity (Chen et al, 2018).

OsFH5 (also named *RMD* and *BUI1*) belongs to type II formin in plant, contains one PTEN (phosphatase and tensin homolog), one FH1 and one FH2 domain (Zhang et al, Yang et al), previous study showed that the mutants showed severe deficiency in most tissues of rice, such as, waved roots, dwarf lines, aberrant seeds shape, stronger sensitivity to gravity (Zhang et al, Huang et al, Song et al, 2019). PTEN domain of formins play important role in attaching with membrane, for instance, plasma membrane and chloroplast, mitochondrion, endoplasmic reticulum and so on (van Gisbergen and Bezanilla, Cvrckova, 2012, Cvrcková, 2013), while FH (formin homology domain)1 is used for binding profilin/actin complex, FH2 is essential for nuclear activity (Cao et al, 2016).

The E3 is an C3HC4 RING finger E3 ligase, named *RIP1* (*RMD/OsFH5* interacting protein 1), also belongs to SINA/SIAH (SINA, seven in absentia; SIAH, seven in absentia homologue) E3 ligases. This kinds of E3 ligases are highly conserved in evolution, not only in animals (Pepper et al, 2017) but also in plants (Den Herder et al, 2008), SINA ubiquitin ligases are members of the RING finger E3 ligases (Qi et al, 2013), RING domain in N terminus is used for binding E2 proteins (Matsuzawa et al, 2003), while the C terminus contains SBS (substrate binding site) and DIMER (the dimerization) domain (Siswanto et al, 2018). SINA E3s engage in a variety of life activities, as drought response in rice (Ning et al, 2011a); SINAT (SINA of Arabidopsis thaliana) 5 influences lateral root number and involved in auxin and brassinosteroid signals in Arabidopsis (Xie et al, 2002, Yang et al, 2017); cold stress in banana (Fan et al, 2017); different types of stress in apple (Li et al, 2020) and the like.

In our research, RIPs were all proved to interact with OsFH5, all can form homo or hetero oligomers and are able to relocate OsFH5, they can slow down degradation rate of OsFH5 in half *in vivo* experiments. *Rips* multi mutants showed serious phenotype as expected, such as dwarf phenotype and seeds defect, which are similar with *osfh5* mutants, microfilaments in *rips* also became tangled compared with wild type. Beyond that, *rips* also exhibit some other specific phenotypes, including the flag leaf angle and primary branch of panicle angle were appreciable enlarged, spiral crimped roots, indicate that *rips* mutant may cause effects on other processes.

Results

OsFH5 interacts with RIP SIAH domains in heterologous systems

To discover proteins that may interact with OsFH5, we used a yeast two hybrid (Y2H) screen with the OsFH5 N-terminal P2 fragment (821 amino acids) as bait (Fig. 1a). The most common interacting protein (63%) was the SIAH domain from RIP1 (Fig. 1b). Further analysis with full-length and truncated OsFH5 and RIP1 constructs confirmed that the SIAH domains from RIP1 interacts with the P3 domain of OsFH5 (aa 338–821), with no currently recognized functional domain (Fig. 1a–c). Intriguingly, full-length OsFH5 could interact with the truncated SIAH domain and the full-length RIP1 protein could interact with the truncated P2 and P3 domains from OsFH5; but the two full-length OsFH5 and RIP1 proteins could not interact in the Y2H assay, suggesting possible steric hindrance of two large proteins interfering with the GAL4 activation domain (Fig. 1c), and though P3 showed self-activating in 3SD medium but not in 4SD medium. However, the full-length proteins were observed to interact in bimolecular fluorescence complementation (BiFC) assays in tobacco leaves (Fig. 1d).

In silico analyses using the full-length RIP1 protein sequence revealed 5 RIP1 homologs in rice (RIP2–6), and six homologs in Arabidopsis. Phylogenetic analysis revealed similar arrangements in the two species, where RIP1, RIP2, and RIP3 orthologs appeared to form one clade, while the remaining 6 proteins (RIP4, RIP5, and RIP6 orthologs) formed a second clade (Fig. 1e). Due to the high homology of rice RIP proteins, we tested whether their SIAH domains could interact with OsFH5, and all 5 SIAH domains

(labelled SIAH2–6 from RIP2–6, respectively) could interact with both P2 fragments and full-length OsFH5 (Figure S1a). Interaction between full-length RIP2,4,5,6 and OsFH5 proteins was verified using BiFC assays in tobacco leaves (Figure S1b); however, cloning of full-length *RIP3* failed, possibly due to high GC content, and its protein expression and interaction assays could not be performed.

RIP proteins can form homo- and hetero-oligomers

Previous reports from Arabidopsis and human systems have indicated that E3 ligases can form dimers, mediated by SIAH domains (Xie et al, 2002, Depaux et al, 2006)., We used both Y2H and BiFC assays to examine whether this function is conserved in rice RIP proteins. Y2H assays revealed that RIP1 could form homo-oligomers when co-expressed with itself or its SIAH1 domain, and with the SIAH domains of the other 5 RIP proteins (Figure 2a). BiFC confirmed that all full-length proteins, when co-expressed either with themselves of with other RIP proteins, also interacted in tobacco leaves (Figure 2b, S2). These results suggest that there may be functional redundancies between rice RIP homologs.

RIPs affect localization of OsFH5

To determine the intracellular location of RIP1, we expressed a RIP1-eGFP fusion protein in rice protoplast. Punctate distribution in the cytoplasm was observed that did not coincide with chloroplasts (Figure 3a), similar to the distribution of the RIP1 homo-oligomer in tobacco leaves (Figure 2b). The GFP-OsFH5 fusion protein also localized to the cytoplasm, but in a more diffuse distribution, and to the plasma membrane, both in rice protoplasts (Figure 3b) and tobacco leaves (Figure 3d). Attempts to co-transfect OsFH5-cYFP with full length RIP1-nYFP into rice protoplasts were unsuccessful, but co-transfection of OsFH5-cYFP and the shorter SIAH1-nYFP revealed protein interaction in the cytoplasm (Figure 3c). into rice protoplast due to hardly successful to co-transfect the result also showed out speckled fluorescence signals in cytoplasm (Figure 3c), similar to the pattern observed with full-length RIP1-eGFP (Figure 3a). To further test this finding, we co-expressed eGFP-OsFH5 and RIP proteins in tobacco leaves, and observed the same punctate distribution in all protein combinations (Figure 3e–i), quite distinct from the pattern observed with eGFP-OsFH5 was expressed by itself (Figure 3d). These results demonstrate that interaction with RIP proteins appears to alter the intracellular distribution of OsFH5.

RIPs inhibit degradation of OsFH5

The known function of RIP proteins as E3 ubiquitin ligases suggests that interaction between RIPs (RIP proteins) and OsFH5 may target OsFH5 for ubiquitin-mediated protein degradation via the proteasome system (Liyuan et al, 2013), so we did degradation experiments. OsFH5 and RIP-eGFP were expressed separately in from tobacco leaves, all proteins were extracted, and then mixed in different ratios. Presence

of the OsFH5 and RIP proteins was detected by anti-OsFH5 and anti-eGFP antibodies, respectively, at 0 min and 10 min after mixing.

In the absence of RIP1, OsFH5 was nearly completely degraded after 10 min (Figure 4a-4c). However, OsFH5 degradation was slowed as RIP1 concentration increased (Figure 4a-c), contrary to expectations that RIP1 would increase OsFH5 degradation. Addition of the proteasome inhibitor MF132 didn't change the pattern (Figure 4a, 4d and 4e), this suggests that RIP1's function is not to degrade OsFH5.

These experiments were repeated using RIP5 or RIP6 instead of RIP1 (Figure S3a and S3d). With the increase of RIP5 and RIP6 concentration, the law that the degradation rate of OsFH5 slowed down did not change (Figure S3b and S3d).

rips mutants have a similar phenotype to *osfh5* mutant plants

To study the functions of RIP proteins *in vivo*, different *RIP* genes were knocked out or overexpressed in transgenic rice. First, *RIP1* knock out (Figure 5c) and overexpression (Figure S4) lines did not show any obvious phenotype. Given the potential for functional redundancy, the *rip2 rip3* double mutant was obtained and also similar to wild type plants (Figure 5c). *rips* (*rip1-rip6* genes) multiple knockout lines were constructed and gained different types mutant lines (Figure 5a and 5b), *rips* mutant lines exhibited significant developmental defects, similar to the *osfh5* mutant: plant height decreased about 25% (Figure 5c and 5d), and mature rice seeds were shorter and less smooth (Figure 5e, S5a–c) than wild type. Leaf width, increased in *osfh5* leaves, was further increased in *rips* leaves (Figure S5d and S5e); lag leaf angle and primary branch of panicle angle were enlarged to varying degrees in *rips* plants (Figure S5f).

Microfilaments organization of *rips* roots became tangled

Unlike *osfh5* roots, *rips* roots were displayed spiral, crinkled growth compared with wild type (Figure 6a, 6b). Given the interaction between RIP proteins and OsFH5, and the role of OsFH5 in microfilament extending and bundling, we examined the morphology of root microfilaments. After staining with phalloidin-488, wild type roots showed clear microfilament morphology, compared with apparently tangled microfilaments in *rips* roots (Figure 6c and 6d), with an obvious increase in actin filament abundance but no measurable change in actin architecture (Figure 6e, 6f). Previous studies have shown that *osfh5* cells exhibit more transversely arranged microfilaments (Zhang et al); our results indicate that RIP proteins may affect microfilament organization through OsFH5-independent pathways.

Discussion

In consideration of conservatism of Siah ubiquitin ligases, one peptide motif PxAxVxP (VxP, core sequence; x, any amino acid) was reported is important for mediating the interaction among SINA type

proteins and a range of partners (House et al, 2003), so we checked partial amino acid sequences of reported SINA target proteins, such as, BES1, BZR1, FREE1, VPS23A and OsNek6, found that they are all contain one or more VxP motif, especially, one PHAHVTP motif was found in VPS23A protein (Yang et al, 2017, Xia et al, 2020, Ning et al, 2011b), and just right, one PKAVKP motif was found in the P3 C-terminal of OsFH5 (Fig. 1a). To prove this, we truncated P2 into P1 and P3, found that P1 can't interacting with RIP1, while on the contrary, P3 can interact with RIP1 (Fig. 1c), this indicate that PTEN domain has no function in terms of protein interactions. Since no other specific domains or elements have been identified on P3 so far and in view of previous studies on SIAH E3 ligases binding substrates, PKAVKP motif may play a key role in mediating the interaction between OsFH5 and RIP1. For SINA ligase proteins, another obvious characteristic is to form homo or hetero oligomers, for instance, MtSINA in Medicago truncatula (Den Herder et al, 2008); SISINA in tomato (Wang et al, 2018); MdSINA2 in apple (Li et al, 2020), and be no exception for RIP proteins in rice, were also confirmed in our study (Fig. 2 and S2).

With regard to the location of SINA type E3 ligase, most are located in nucleus (Table 1), but different proteins are different in plant. In Arabidopsis, SINATs, homologous *of RIP1*, were reported to locate in nucleus and cytoplasm (Yang et al, 2017); and also for SINAL7, but nuclear localization is required (Peralta et al, 2016); another report described SINATs primarily localized to the endosomal and autophagic vesicles (Xia et al, 2020); MdSINA2 of apple was found to be localized in the nucleus as well (Li et al, 2020); OsDIS1 of rice localized predominantly in the nucleus (Ning et al, 2011b); OsHIR1 localizes to the plasma membrane and nucleus (Lim et al, 2014), also some researches are reported to involved in influence on target proteins localization. In one another investigation showed that SINA4 localized in the cytosol and/or cytosolic dots of variable size and could relocate SYMRK in Lotus japonicus (Den Herder et al, 2012), SINAT5 could relocate FLC into nuclear bodies (Park et al, 2007), and from that point of view, RIPs have same function on changing localization of target protein OsFH5 (Fig. 3), and that, one report in budding yeast, two RING type E3, Dma1 and Dma2 are required for proper formin localization (Juanes and Piatti, 2016).

Most report on function of SIAH ubiquitin ligases are about mediating degradation of target proteins to participate in various organic activities in plant (Table 1) (Zhang et al, 2019), like OsDIS1 degrade OsNek6 via the 26S proteasome-dependent pathway to regulate drought response and $OsHIR_1$ positive regulates arsenic and cadmium metal in rice (Ning et al, 2011b, Lim et al, 2014); SINAT E3 ubiquitin ligases not only mediate FREE1 and VPS23A degradation to modulate abscisic acid signaling but also regulate the stability of the ESCRT component FREE1 in response to iron deficiency in Arabidopsis (Xia et al, 2020, Xiao et al, 2020); banana fruit SINA ubiquitin ligase MaSINA1 regulates the stability of MaICE1 to be negatively involved in cold stress response (Fan et al, 2017) and the like. There is, however, a report described that DET1 inhibits LHY proteolytic turnover which ubiquitinated by SINAT5 in Arabidopsis, DET1 is also a substrate for SINAT5 but can't be ubiquitinated (Park et al, 2010). In our investigation, given the big relative molecular weight of OsFH5 (about 180kd), both detection of changes in OsFH5 protein levels *in vivo* and ubiquitination experiment *in vitro* are failed maybe due to difficulty extraction and purification of large and proline enriched proteins, so we adopted another methods degradation

experiment, found that OsFH5 protein degradation directly were slowed down as RIPs concentration increases, indicate that RIPs not only involved in slow OsFH5 degradation rate but also maybe improved the stability by emulative interaction and/or ubiquitination, or through the influence on the OsFH5 localization in vivo, and phenotypes shown of *rips* seems also proved this in some way.

Table 1
SIAH E3 ligase research progress in plants

Gene	Species	Location	Substrate	Function
OsDIS1 (Ning et al, 2011a)	rice	nucleus	OsNek6	degradation
$OsHIR_1$ (Lim et al, 2014)	rice	plasma membrane, nucleus	OsTIP4;1	degradation
SINAT E3 (Xia et al, 2020)	Arabidopsis	punctate structures in the cytoplasm, nucleus	FREE1, VPS23A	degradation
MaSINA1 (Fan et al, 2017)	banana	nucleus	MaICE1	degradation
SINAT5 (Park et al, 2010, Park et al, 2007)	Arabidopsis	nuclear body	LHY, DET1	LHY is a substrate of SINAT5, DET1 inhibits E3 ubiquitin ligase activity of SINAT5
MdSINA2 (Li et al, 2020)	apple	nucleus	-	-
SINA4 (Den Herder et al, 2012)	Lotus japonicus	punctae at the cytosolic interface of plasma membrane	SYMRK	affects SYMRK stability
"-" means none reported.				

In addition, *rips* also showed some very different phenotypes that didn't found in *osfh5*, for instance, angle between leaf, primary branches and stems were enlarged (Figure S5f); the *rips* roots bend like twine and circle of curls especially in root tips. The reason caused these results may be due to effect on the expression of other genes. Sometimes E3 ligases are not limited to a single substrate, although it is specific for substrate recognition, like OsDIS1, not only plays a negative role in drought stress tolerance possibly through the posttranslational regulation of OsNek6 but also interacts with OsSKIPa, a drought and salt stress positive regulator in rice (Ning et al, 2011c); SINAT E3 ubiquitin ligases mediate both FREE1 and VPS23A degradation to participate in different regulatory pathways (Xia et al, 2020, Xiao et al, 2020). Given the complexity of regulatory networks in organisms, most often the same gene may also be involved in different regulatory progresses, such as, RING finger ubiquitin E3 ligase SDIR1 targets SDIR1-INTERACTING PROTEIN1 for degradation not only to modulate the salt stress response but also ABA signaling in Arabidopsis (Zhang et al, 2015).

Conclusions

In summary, our research uncovered SINA protein RIP1 and homologous genes RIP2-RIP6, which can form homo- and hetero- oligomers, to relocate OsFH5 by interactions, and control the morphology of rice by inhibiting OsFH5 degradation.

Abbreviations

SUMO
small ubiquitin-like modifier
NEDD
neural precursor cell-expressed developmentally down-regulated
ATG
autophagy-related gene
PTEN
phosphatase and tensin homolog
FH
formin homology domain
SINA
seven in absentia
SIAH
seven in absentia homologue
RMD
rice morphology determinant
BUI1
bent uppermost internode1
RIP
RMD interacting protein
RIPs
RIP proteins
Y2H
yeast two hybrid
BiFC
bimolecular fluorescence complementation

Methods

Mutant materials and growth conditions

Wild type rice (*Oryza sativa* cv. 9522) and mutant plants were grown in the paddy fields of Shanghai Jiao Tong University (30 °N 121 °E) from June to September (the natural growing season) according to

standard local practice. Stem lengths were measured, and grains were harvested, at maturity. Differences in mature plant height, flag leaf width (7-day old seedlings) and seed length/width were analyzed using ruler and Excel. The *osfh5* mutant in the 9522 background was available from previous work (Zhang et al., 2011). The *rip1*, *rip2 rip3* and *rips* mutants were generated in 9522 via CRISPR-Cas9 as previously described (Xie et al, 2015). CRISPR-Cas9 guide RNAs and screening primers are shown in Table S1.

Yeast two hybrid (Y2H) assays

Yeast two hybrid experiments were performed according to the manufacturer's instructions (Clontech). The coding sequences of *OsFH5*, *P1*, *P2* and *P3* were fused in-frame with the sequence encoding the GAL4 DNA-binding domain of the bait vector pGBKT7 (BK). The coding sequences of *RIP1* and *SIAH1* were cloned in the prey vector pGADT7 (AD). Primers for cloning are given in Table S1. Each bait–prey pair was co-transformed into *Saccharomyces cerevisiae* strain AH109 as previously described (Lecrenier et al, 1998). Yeast was grown for 2–3 days in liquid YPDA medium (Yeast Extract Peptone Dextrose Medium) at 28°C, then dilutions were spotted onto selective SD media containing 20 mg/ml X-gal, and grown for a further 2–3 days. Three amino acid–-deficient medium (–his –leu –trp) and four amino acid–deficient medium (–his –leu –trp –ade) was used to test the binding ability of protein interaction.

To analyze formation of homo- and hetero-oligomers between RIP proteins, *RIP1* was cloned into pGBKT7, and paired with prey vectors (pGADT7) encoding SIAH1–6 domains from RIP1 to RIP6, respectively. Transfection and selective growth as above.

Bimolecular fluorescence complementation (BiFC)

DNA encoding *RIP1*–*RIP6*, *SIAH1*, and *OsFH5* were amplified and fused with nYFP, cYFP, and/or eGFP, cloned into pXY104 and pXY106 vectors (From Prof. Hongquan Yang's Lab of SJTU), using primers shown in Table S1. Constructs were individually or co-transformed into 2-day *Nicotiana benthamiana* leaves using Agrobacterium-mediated transformation as previously described (Li et al, 2017). After 24–36 h in the dark, tobacco leaf cells were observed under 50 % glycerol with a Leica sp5 confocal laser scanning microscope.

Phylogenetic analyses

The RIP1 protein sequence was used for BLASTp screening of other proteins from National Center for Biotechnology Information (NCBI) and https://www.arabidopsis.org/. Matching protein sequences were aligned with the software Molecular Evolutionary Genetics Analysis (MEGA) and used to create an evolutionary tree. Branch support was assessed with 1000 bootstrap replicates (Felsenstein, 1985, Sanderson and Wojciechowski, 2000).

Transient gene expression in rice protoplasts

Rice protoplasts were prepared according to Zhang et al (2011) with the following modifications. Wild type 9522 seeds were germinated in dark for 2 weeks in the dark. 50–60 seedlings (no seeds) were

harvested, cut into 0.5 mm lengths, and incubated in 0.6 M mannitol in the dark for 10 min. The mannitol solution was discarded and replaced with enzymatic solution (1.5 % (w/w) cellulase RS, 0.75 % (w/w) macerozyme R-10, 0.6 M mannitol, 10 mM MES (pH 5.7), 10mM $CaCl_2$ and 0.1 % BSA), and vacuum infiltrated for 1 h, before shaking at 60–80 rpm in the dark for 4–5 h in room temperature. The enzymatic hydrolysate was removed by 1ml syringe. Cells were gently resuspended in W5 solution (154 mM NaCl, 125 mM $CaCl_2$, 5 mM KCl and 2 mM MES (pH 5.7)), and the protoplasts were released after shaking at room temperature for 1 h in dark. Protoplasts were collected after filtrated into small bottles through 40μm nylon mesh (Millipore) and washed 3 times with fresh W5 solution at 1500 *RPM* for 3 min. Protoplasts were collected and precipitated with an appropriate amount of MMG solution (0.4 M mannitol, 15 mM $MgCl_2$ and 4 mM MES (pH 5.7)), and resuspended to a concentration of 2×10^6 cells/ml in room temperature.

For transient protoplast transformation, 10 μg of plasmid DNA and 200 μl of protoplast solution were combined in a 2 ml Eppendorf tube, to which 220 μl (w/v) PEG was gentled added, and mixed gently at room temperature for 20 min. 1 ml of W5 solution was added, and protoplasts gently pelleted at 200 *g* for 1 min. The supernatant was discarded, and 1 ml W5 solution was used to resuspend the protoplasts and transfer them to a 12-well plate (moistened in advance with 1 mL 5% BSA). Plates were incubated in the dark at 22°C overnight, and again pelleted gently at 200 *g* for 1 min. The supernatant was discarded, and the fluorescence signal was observed by confocal fluorescence microscopy, eGFP excitation is 488 nm, YFP excitation is 514 nm, chloroplasts can fluoresce spontaneously.

In vitro **protein stability assays**

Protein expression expressing OsFH5, RIP1-eGFP, RIP5-eGFP, and RIP6-eGFP were introduced separately into *N. benthamiana* leaves via *Agrobacterium*-mediated transformation, as described above. After 36–48 h in the dark, tobacco leaves were harvested, ground under liquid nitrogen, and extracted with a non-denaturing extraction buffer (50 mM Tris-MES (pH 8.0), 0.5 M sucrose, 1 mM $MgCl_2$, 10 mM EDTA, 5 mM DTT, protease inhibitor cocktail (Sigma, 1 complete Mini tablet per 10 ml of extraction buffer)).

OsFH5 extract was mixed with different ratios (0, 1, 2, 4, or 8× vol) of RIP1 extract, and incubated to 0 min, or for 10 min at room temperature in the presence and absence of 20 μM MG132 (Sigma), a proteosome inhibitor. A OsFH5 negative control was also used (a 9× vol of RIP1 extract). Mixtures were immediately run on a protein gel, transferred to a western blot, and probed with anti-OsFH5 antibody (Zhang et al) or anti-eGFP antibody to detect RIP protein, as previously described.

Root and microfilament observation

Roots from 3 d seedlings grown in light incubator were used for picture with Asana mirror (Leica). Microfilaments from cv. 9522 and *rips* roots were stained using the glycerol method (Olysla egers and Verbelen, 1998). Roots from 3 d seedlings grown in light incubator were incubated in PEM buffer (100 mM PIPES, 10 mM EGTA, 5 mM $MgSO_4$, and 0.3 M mannitol, pH 6.9) that contains 1% (w/v) glycerol

(Sigma Aldrich) and 6.6 mM Alexa Fluor 488-phalloidin staining (Invitrogen). After a 30 min incubation, root tips were observed in 50% glycerol with a Leica TCS SP5 confocal laser scanning microscope equipped with a 363 1.46–numerical aperture HC PLANs objective to determine microfilament lengths in lateral root cells. Actin filament abundance and bundling (skewness) were measured using image J.

Accession numbers

RIP1, Os02g0293400; *RIP2*, Os05g0238200; *RIP3*, Os01g0234900; *RIP4*, Os02g0128800; *RIP5*, Os03g0356414; *RIP6*, l Os07g0659800. Arabidopsis *RIP* homologs: At2g41980, At3g13672, At3g58040, At5g53360, At4g27880, At3g61790.

Declarations

Ethics declarations

Ethics Approval and Consent to Participate

Not applicable.

Consent for Publication

Not applicable.

Availability of supporting data

The datasets supporting the conclusions of this article are provided within the article and its additional files.

Competing interests

The authors declare that they have no competing interests.

Funding

This work was supported by the National Key Research and Development Program of China (2016YFD0100804 and 2016YFD0100903), the National Natural Science Foundation of China (31861163002 and 31700276), the Innovative Research Team, Ministry of Education, and 111 Project (B14016).

Authors' Contributions

Shuwei Chang and Dabing Zhang conceived and designed the experiments. Guoqiang Huang, Duoxiang Wang, Wanwan Zhu helped with the experiment. Litao Yang, Wanqi Liang, Qi Xie offered suggestion. Shuwei Chang wrote the paper. Dabing Zhang revised the paper. All authors read and approved the manuscript.

Acknowledgements

We thank Ms Xiaofei Chen for the help provided in rice transgenic seedling culture; Ms Mingjiao Chen and Mr Zhijing Luo for assistance with rice cultivation; and Prof. Qi Xie for protein extraction buffer. This work was supported by the National Key Research and Development Program of China (2016YFD0100804 and 2016YFD0100903), the National Natural Science Foundation of China (31861163002 and 31700276), the Innovative Research Team, Ministry of Education, and 111 Project (B14016).

References

1. Bu F., Yang M., Guo X., Huang W., Chen L. 2020. Multiple Functions of ATG8 Family Proteins in Plant Autophagy. Front Cell Dev Biol, 8: 466.
2. Buetow L., Huang D. T. 2016. Structural insights into the catalysis and regulation of E3 ubiquitin ligases. Nat Rev Mol Cell Biol, 17(10): 626-642.
3. Cao L., Henty-Ridilla J. L., Blanchoin L., Staiger C. J. 2016. Profilin-Dependent Nucleation and Assembly of Actin Filaments Controls Cell Elongation in Arabidopsis. Plant Physiol, 170(1): 220-233.
4. Chen Y., Fokar M., Kang M., Chen N., Allen R. D., Chen Y. 2018. Phosphorylation of Arabidopsis SINA2 by CDKG1 affects its ubiquitin ligase activity. BMC Plant Biol, 18(1): 147.
5. Cvrckova F. 2012. Formins: emerging players in the dynamic plant cell cortex. Scientifica (Cairo), 2012: 712605.
6. Cvrckova Fatima. 2013. Formins and membranes: anchoring cortical actin to the cell wall and beyond. FRONT PLANT SCI, 4: 436.
7. Den Herder G., De Keyser A., De Rycke R., Rombauts S., Van de Velde W., Clemente M. R., Verplancke C., Mergaert P., Kondorosi E., Holsters M., Goormachtig S. 2008. Seven in absentia proteins affect plant growth and nodulation in Medicago truncatula. Plant Physiol, 148(1): 369-382.
8. Den Herder G., Yoshida S., Antolin-Llovera M., Ried M. K., Parniske M. 2012. Lotus japonicus E3 ligase SEVEN IN ABSENTIA4 destabilizes the symbiosis receptor-like kinase SYMRK and negatively regulates rhizobial infection. Plant Cell, 24(4): 1691-1707.
9. Depaux A., Regnier-Ricard F., Germani A., Varin-Blank N. 2006. Dimerization of hSiah proteins regulates their stability. BIOCHEM BIOPH RES CO, 348(3): 857-863.

10. Fan Z. Q., Chen J. Y., Kuang J. F., Lu W. J., Shan W. 2017. The Banana Fruit SINA Ubiquitin Ligase MaSINA1 Regulates the Stability of MaICE1 to be Negatively Involved in Cold Stress Response. Front Plant Sci, 8: 995.
11. Felsenstein J. 1985. Confidence Limits on Phylogenies: An Approach Using the Bootstrap. Evolution, 39(4): 783-791.
12. French M. E., Koehler C. F., Hunter T. 2021. Emerging functions of branched ubiquitin chains. Cell Discov, 7(1): 6.
13. Ghimire Shantwana, Tang Xun, Zhang Ning, Liu Weigang, Si Huaijun 2020. SUMO and SUMOylation in plant abiotic stress. PLANT GROWTH REGUL, 91: 317-325.
14. House C. M., Frew I. J., Huang H. L., Wiche G., Traficante N., Nice E., Catimel B., Bowtell D. D. 2003. A binding motif for Siah ubiquitin ligase. Proc Natl Acad Sci U S A, 100(6): 3101-3106.
15. Huang Guoqiang, Wanqi Liang, J. Sturrock Craig, K. Pandey Bipin, Jitender Giri, Stefan Mairhofer, Daoyang Wang, Lukas Muller, Hexin Tan, Communications York Larry M. 2018. Rice actin binding protein RMD controls crown root angle in response to external phosphate. NAT COMMUN, 9(1): 2346-.
16. Juanes M. A., Piatti S. 2016. Control of Formin Distribution and Actin Cable Assembly by the E3 Ubiquitin Ligases Dma1 and Dma2. Genetics, 204(1): 205-220.
17. Lecrenier N., Foury F., Goffeau A. 1998. Two hybrid systematic screening of the yeast proteome. Bioessays, 20(1): 1-5.
18. Li H. L., Wang X., Ji X. L., Qiao Z. W., You C. X., Hao Y. J. 2020. Genome-Wide Identification of Apple Ubiquitin SINA E3 Ligase and Functional Characterization of MdSINA2. Front Plant Sci, 11: 1109.
19. Li W., Cao J. Y., Xu Y. P., Cai X. Z. 2017. Artificial Agrobacterium tumefaciens strains exhibit diverse mechanisms to repress Xanthomonas oryzae pv. oryzae-induced hypersensitive response and non-host resistance in Nicotiana benthamiana. Mol Plant Pathol, 18(4): 489-502.
20. Lim S. D., Hwang J. G., Han A. R., Park Y. C., Lee C., Ok Y. S., Jang C. S. 2014. Positive regulation of rice RING E3 ligase OsHIR1 in arsenic and cadmium uptakes. Plant Mol Biol, 85(4-5): 365-379.
21. Liyuan, Chen, Hanjo, Hellmann 2013. Plant E3 Ligases: Flexible Enzymes in a Sessile World. Mol Plant, 6(5): 1388-1404.
22. Matsuzawa., Shu ichi., Chenglong Li., Chao Zhou., Ni., Takayama., Shinichi., Reed., John. 2003. Structural Analysis of Siah1 and Its Interactions with Siah-interacting Protein (SIP). J Biol Chem, 278(3): 1837-1840.
23. Mazzucotelli E., Belloni S., Marone D., De Leonardis A., Guerra D., Di Fonzo N., Cattivelli L., Mastrangelo A. 2006a. The e3 ubiquitin ligase gene family in plants: regulation by degradation. Curr Genomics, 7(8): 509-522.
24. Mazzucotelli E., Belloni S., Marone D., De Leonardis A. M., Guerra D., Fonzo N., Cattivelli L., Mastrangelo A. M. 2006b. The E3 ubiquitin ligase gene family in plants: Regulation by degradation. Curr Genomics, 7(8): 509-522.

25. Mergner J., Schwechheimer C. 2014. The NEDD8 modification pathway in plants. Front Plant Sci, 5: 103.
26. Michael, J., Clague, Claire, Heride, Sylvie, Urbé. 2015. The demographics of the ubiquitin system. Trends Cell Biol, 25(7): 417-426.
27. Miura K., Hasegawa P. M. 2010. Sumoylation and other ubiquitin-like post-translational modifications in plants. Trends Cell Biol, 20(4): 223-232.
28. Nakazawa Y., Hara Y., Oka Y., Komine O., van den Heuvel D., Guo C., Daigaku Y., Isono M., He Y., Shimada M., Kato K., Jia N., Hashimoto S., Kotani Y., Miyoshi Y., Tanaka M., Sobue A., Mitsutake N., Suganami T., Masuda A., Ohno K., Nakada S., Mashimo T., Yamanaka K., Luijsterburg M. S., Ogi T. 2020. Ubiquitination of DNA Damage-Stalled RNAPII Promotes Transcription-Coupled Repair. Cell, 180(6): 1228-1244 e1224.
29. Ning Y., Jantasuriyarat C., Zhao Q., Zhang H., Chen S., Liu J., Liu L., Tang S., Park C. H., Wang X., Liu X., Dai L., Xie Q., Wang G. L. 2011a. The SINA E3 ligase OsDIS1 negatively regulates drought response in rice. Plant Physiol, 157(1): 242-255.
30. Ning Y. S., Jantasuriyarat C., Zhao Q. Z., Zhang H. W., Chen S. B., Liu J. L., Liu L. J., Tang S. Y., Park C. H., Wang X. J., Liu X. L., Dai L. Y., Xie Q., Wang G. L. 2011b. The SINA E3 Ligase OsDIS1 Negatively Regulates Drought Response in Rice. Plant Physiol, 157(1): 242-255.
31. Ning Y., Xie Q., Wang G. L. 2011c. OsDIS1-mediated stress response pathway in rice. Plant Signal Behav, 6(11): 1684-1686.
32. Park B. S., Eo H. J., Jang I. C., Kang H. G., Song J. T., Seo H. S. 2010. Ubiquitination of LHY by SINAT5 regulates flowering time and is inhibited by DET1. Biochem Biophys Res Commun, 398(2): 242-246.
33. Park B. S., Sang W. G., Yeu S. Y., Do Choi Y., Paek N. C., Kim M. C., Song J. T., Seo H. S. 2007. Post-translational regulation of FLC is mediated by an E3 ubiquitin ligase activity of SINAT5 in Arabidopsis. PLANT SCI, 173(2): 269-275.
34. Pepper I. J., Van Sciver R. E., Tang A. H. 2017. Phylogenetic analysis of the SINA/SIAH ubiquitin E3 ligase family in Metazoa. BMC Evol Biol, 17(1): 182.
35. Peralta D. A., Araya A., Busi M. V., Gomez-Casati D. F. 2016. The E3 ubiquitin-ligase SEVEN IN ABSENTIA like 7 mono-ubiquitinates glyceraldehyde-3-phosphate dehydrogenase 1 isoform in vitro and is required for its nuclear localization in Arabidopsis thaliana. Int J Biochem Cell Biol, 70: 48-56.
36. Qi J., Kim H., Scortegagna M., Ronai Z. A. 2013. Regulators and effectors of Siah ubiquitin ligases. Cell Biochem Biophys, 67(1): 15-24.
37. Sanderson M. J., Wojciechowski M. F. 2000. Improved bootstrap confidence limits in large-scale phylogenies, with an example from Neo-Astragalus (Leguminosae). Syst Biol, 49(4): 671-685.
38. Siswanto F. M., Jawi I. M., Kartiko B. H. 2018. The role of E3 ubiquitin ligase seven in absentia homolog in the innate immune system: An overview. Vet World, 11(11): 1551-1557.
39. Song Yu., Li Gang., Nowak Jacqueline., Zhang Xiaoqing., Dabing Zhang. 2019. The Rice Actin-Binding Protein RMD Regulates Light-Dependent Shoot Gravitropism. Plant Physiol 181(2): pp.00497.02019.

40. Swatek K. N., Komander D. 2016. Ubiquitin modifications. Cell Res, 26(4): 399-422.
41. van Gisbergen Peter A.C., Bezanilla Magdalena Plant formins: membrane anchors for actin polymerization. Trends Cell Biol, 23(5): 227-233.
42. Wang W., Fan Y., Niu X., Miao M., Kud J., Zhou B., Zeng L., Liu Y., Xiao F. 2018. Functional analysis of the seven in absentia ubiquitin ligase family in tomato. Plant Cell Environ, 41(3): 689-703.
43. Xia F. N., Zeng B., Liu H. S., Qi H., Xie L. J., Yu L. J., Chen Q. F., Li J. F., Chen Y. Q., Jiang L., Xiao S. 2020. SINAT E3 Ubiquitin Ligases Mediate FREE1 and VPS23A Degradation to Modulate Abscisic Acid Signaling. Plant Cell, 32(10): 3290-3310.
44. Xiao Z., Yang C., Liu C., Yang L., Yang S., Zhou J., Li F., Jiang L., Xiao S., Gao C., Shen W. 2020. SINAT E3 ligases regulate the stability of the ESCRT component FREE1 in response to iron deficiency in plants. J Integr Plant Biol, 62(9): 1399-1417.
45. Xie K., Minkenberg B., Yang Y. 2015. Boosting CRISPR/Cas9 multiplex editing capability with the endogenous tRNA-processing system. Proc Natl Acad Sci U S A, 112(11): 3570-3575.
46. Xie Q., Guo H. S., Dallman G., Fang S., Weissman A. M., Chua N. H. 2002. SINAT5 promotes ubiquitin-related degradation of NAC1 to attenuate auxin signals. Nature, 419(6903): 167-170.
47. Yang M., Li C., Cai Z., Hu Y., Nolan T., Yu F., Yin Y., Xie Q., Tang G., Wang X. 2017. SINAT E3 Ligases Control the Light-Mediated Stability of the Brassinosteroid-Activated Transcription Factor BES1 in Arabidopsis. Dev Cell, 41(1): 47-58 e44.
48. Yang W., Ren S., Zhang X., Gao M., Ye S., Qi Y., Zheng Y., Wang J., Zeng L., Li Q. BENT UPPERMOST INTERNODE1 Encodes the Class II Formin FH5 Crucial for Actin Organization and Rice Development. Plant Cell, 23(2): 661-680.
49. Zhang C., Hao Z., Ning Y., Wang G. L. 2019. SINA E3 Ubiquitin Ligases: Versatile Moderators of Plant Growth and Stress Response. Mol Plant, 12(5): 610-612.
50. Zhang H., Cui F., Wu Y., Lou L., Liu L., Tian M., Ning Y., Shu K., Tang S., Xie Q. 2015. The RING finger ubiquitin E3 ligase SDIR1 targets SDIR1-INTERACTING PROTEIN1 for degradation to modulate the salt stress response and ABA signaling in Arabidopsis. Plant Cell, 27(1): 214-227.
51. Zhang Y., Su J., Duan S., Ao Y., Dai J., Liu J., Wang P., Li Y., Liu B., Feng D., Wang J., Wang H. 2011. A highly efficient rice green tissue protoplast system for transient gene expression and studying light/chloroplast-related processes. Plant Methods, 7(1): 30.
52. Zhang Z., Zhang Y., Tan H., Wang Y., Li G., Liang W., Yuan Z., Hu J., Ren H., Zhang D. RICE MORPHOLOGY DETERMINANT Encodes the Type II Formin FH5 and Regulates Rice Morphogenesis. Plant Cell, 23(2): 681-700.

Figures

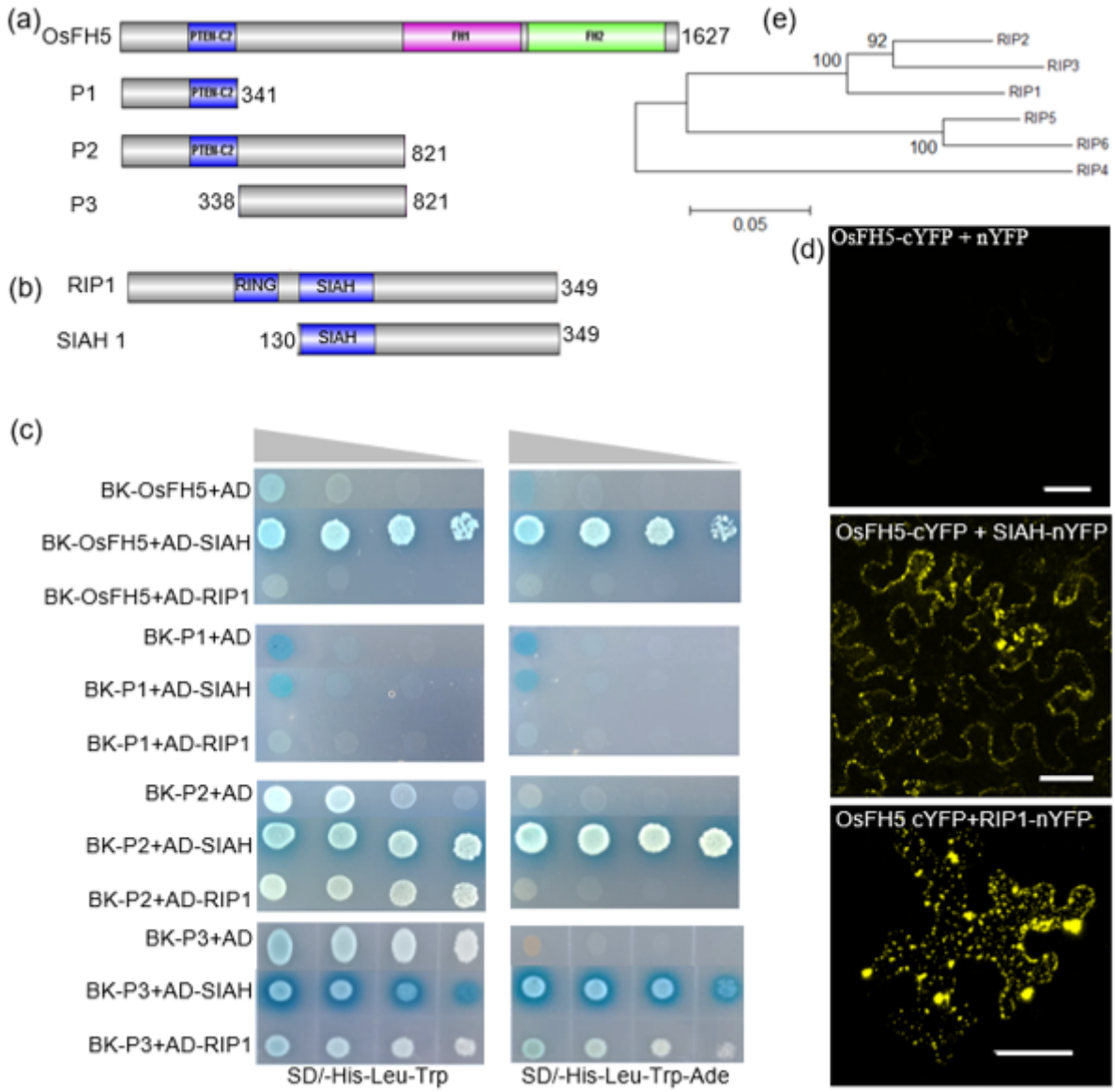

Figure 1

The SIAH domain of RIP1 protein interacts with OsFH5. (a) Full-length OsFH5 protein, indicating PTEN-C2, FH1, and FH2 domains, and the three truncated P1, P2, and P3 constructs. (b) Full-length RIP1 protein, indicating RING and SIAH domains, and the truncated SIAH 1 construct. (c) Yeast 2 hybrid (Y2H) experiment, combining OsFH5 full-length and truncated proteins expressed from the BK bait vector (pGBKT7), and RIP1/SIAH1 proteins expressed from the AD prey vector (pGADT7). Yeast cells co-transformed with each bait–prey pair were grown on selective medium, revealing that the P3 section of OsFH5 is essential for interactions with the RIP1 SIAH1 domain. (d) Bimolecular fluorescence complementation (BiFC) in tobacco leaves reveals that OsFH5 interacts with the SIAH1 domain and full length RIP1. Bar = 50 μm. (e) Phylogenetic tree of rice RIP proteins. Bootstrap support values are indicated on nodes (%).

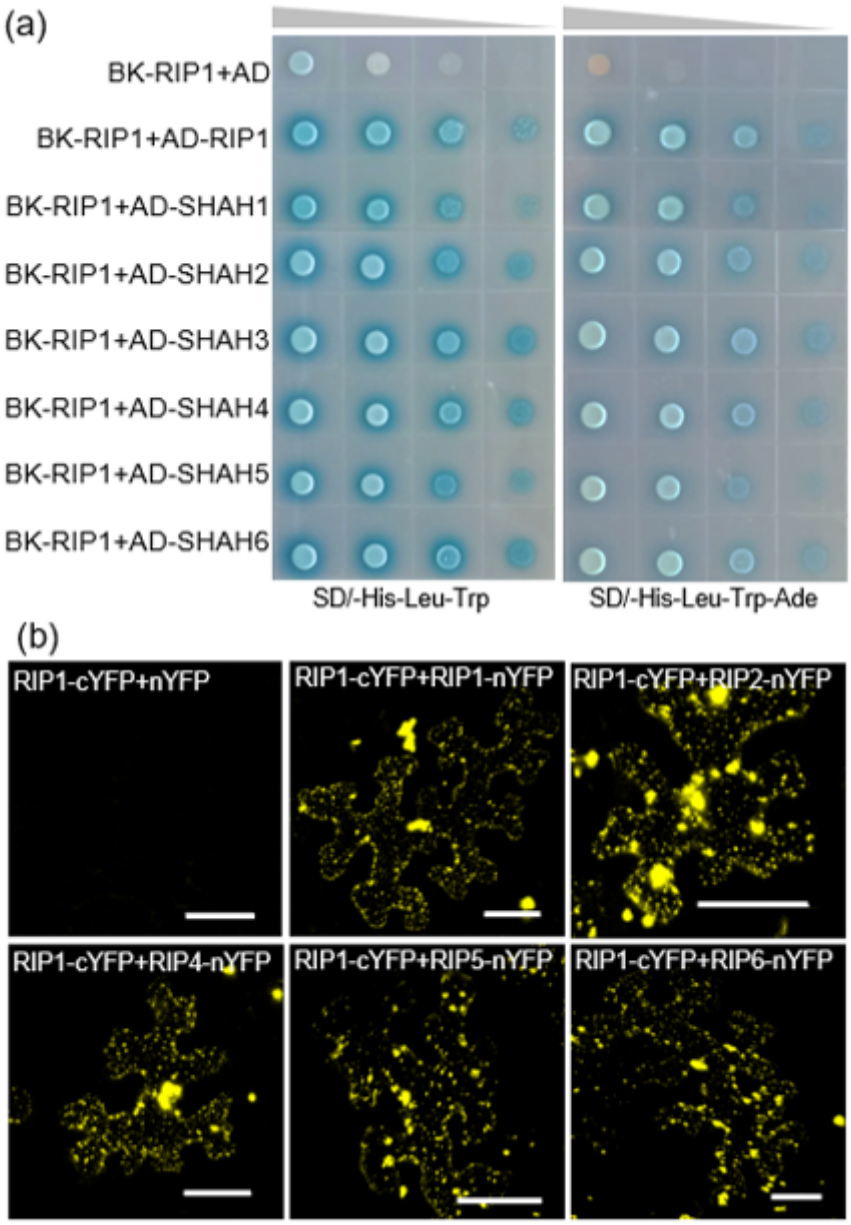

Figure 2

RIP1 forms oligomers with itself and its homologs via SIAH domains. (a) Y2H assays between full-length RIP1 and itself, SIAH1, and SIAH domains from RIP2–RIP6 proteins. (b) BiFC assays confirm that full-length RIP1 (fused to cYFP) interacts with other full-length RIP proteins (fused to nYFP) in tobacco leaves. Bar = 50μm.

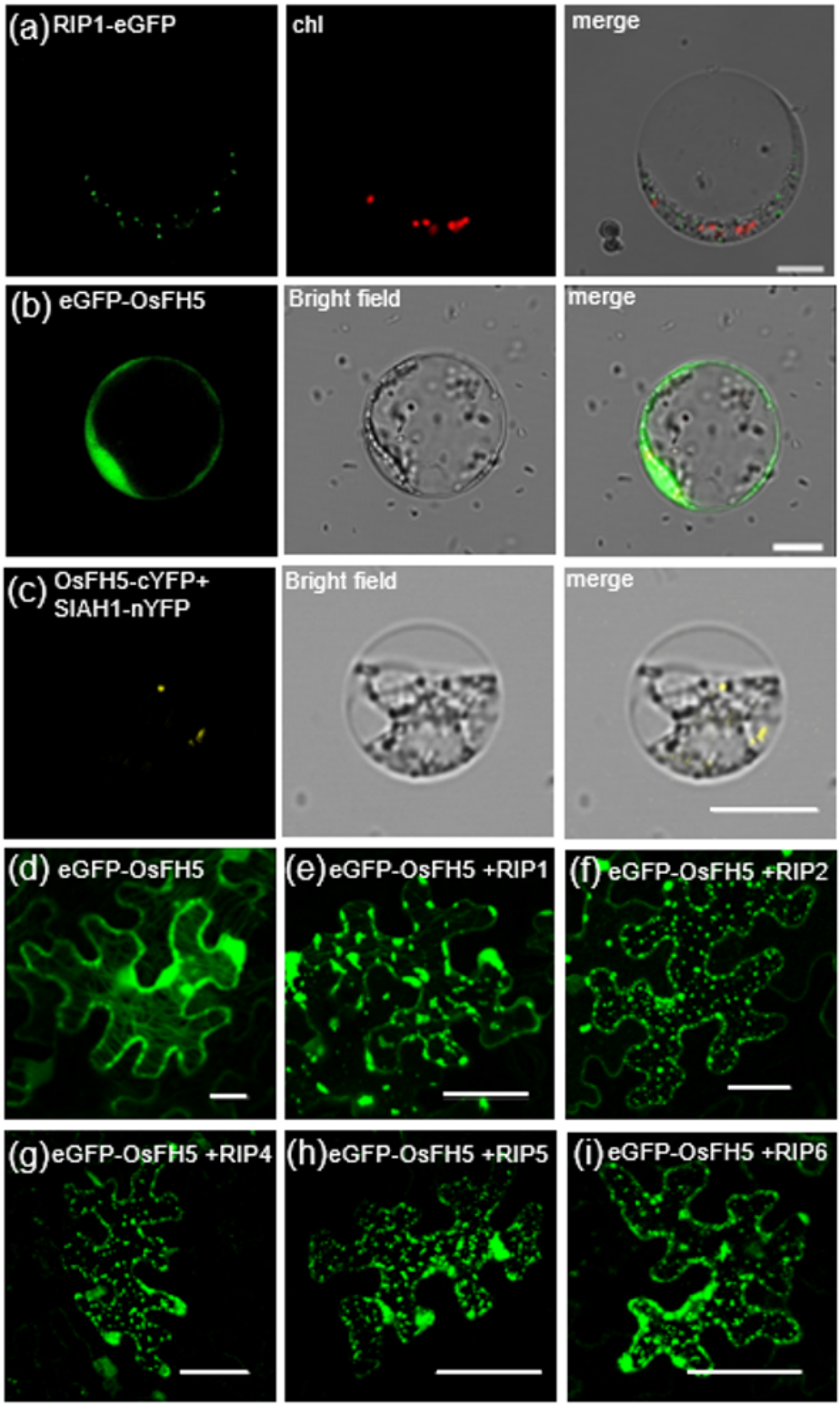

Figure 3

Interaction with RIP proteins influences OsFH5 intracellular localization. (a) RIP1-eGFP, expressed in rice protoplasts, exhibits punctate distribution in the cytoplasm, distinct from chloroplasts (chl) indicated in red via autofluorescence. Bar = 10μm. (b) eGFP-OsFH5, expressed in rice protoplasts, occurs diffusely in the cytoplasm and plasma membrane. Bar=10μm. (c) BiFC reveals that OsFH5 and SIAH1 interact when co-expressed in rice protoplasts. Bar = 10μm. (d) eGFP-OsFH5, expressed in tobacco leaves, occurs

diffusely in the cytoplasm and plasma membrane. Bar = 50μm. (e–i) eGFP-OsFH5, co-expressed with either RIP1, RIP2, RIP4, RIP5, or RIP6 in tobacco leaves, exhibits punctate distribution in the cytoplasm. Bar = 50μm.

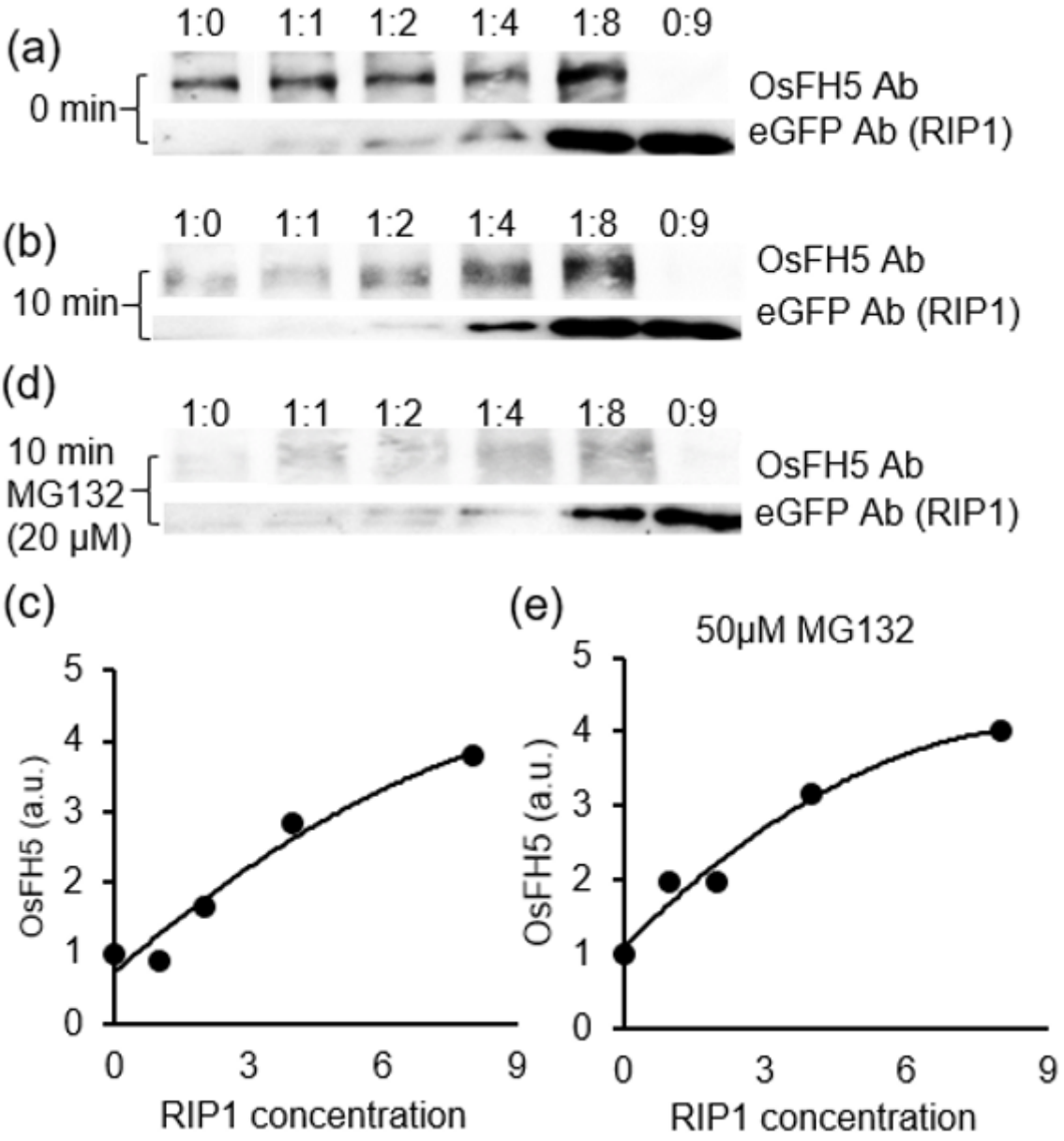

Figure 4

RIP1 inhibits degradation of the OsFH5 protein. OsFH5 protein extract was mixed with different ratios (0, 1, 2, 4, or 8× vol) of RIP1-eGFP extract. The sixth lane contains a 9×vol of RIP1 extract with no OsFH5 extract. Anti-OsFH5 antibody (Ab) was used to detect osFH5; anti-eGFP antibody was used to detect tagged RIP1. (a) Protein amounts immediately after mixing (0 min). (b) Protein amounts 10 min after mixing. (c) Data statistic of OsFH5 10 min from (b). a.u., arbitrary unit. (d) Protein amounts 10 min after mixing in the presence of MG132, a proteasome inhibitor. (e) Data statistic of OsFH5 10 min from (d). a.u., arbitrary unit.

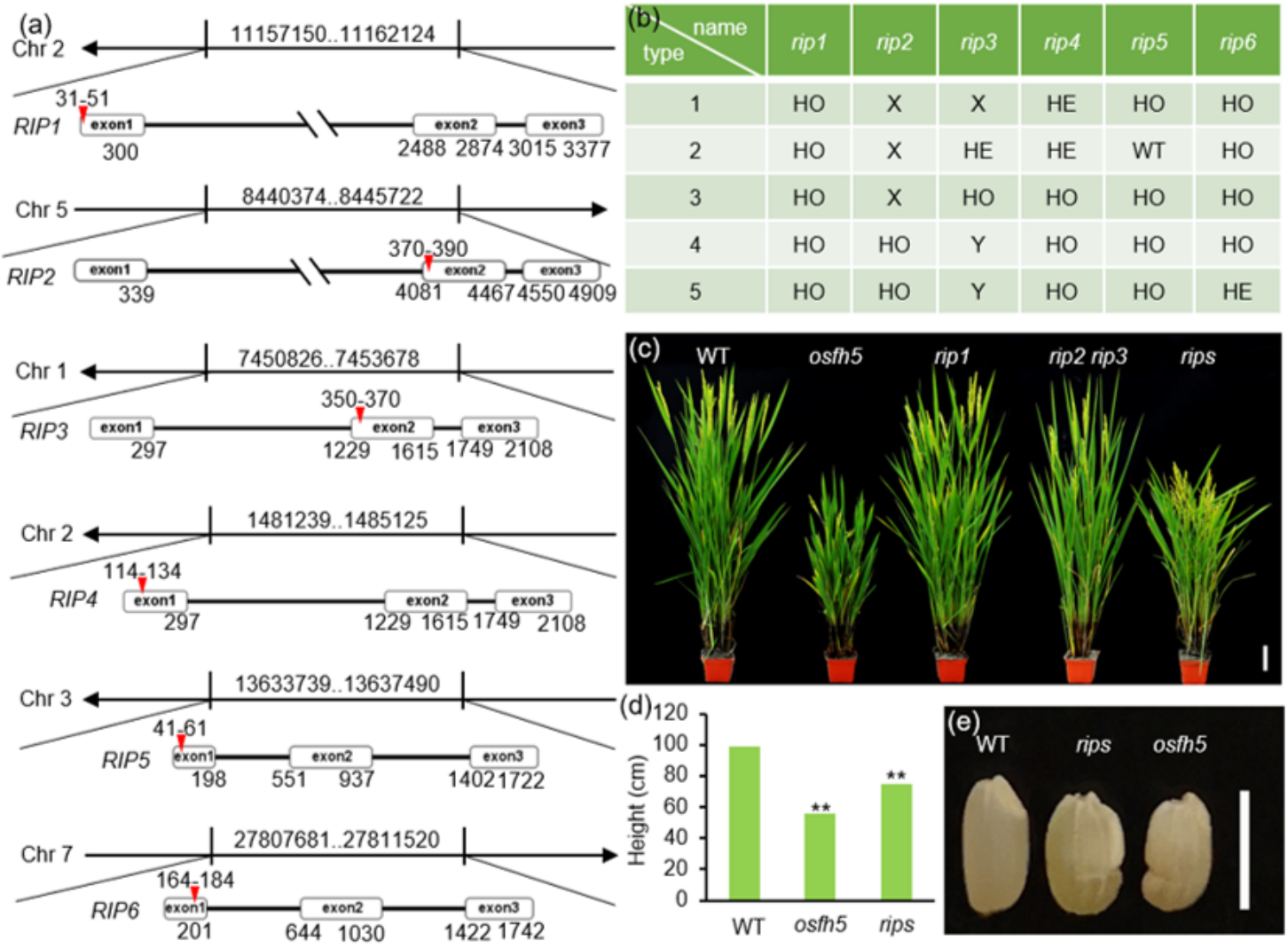

Figure 5

Construction and phenotypes of rip single, double and multi-knockout lines. (a) All 6 RIP genes contain three exons. Mutation sites (CRISPR) are marked with red triangles; the arrow represents the plus and minus strands of the chromosome (Chr.). (b) Five independent mutants were generated for each RIP gene. HO, homozygote; HE, heterozygote; X, amino acid(s) deletion; Y, detected many times but unsuccessfully. (c) Phenotype of about 3-months old rip1, rip2 rip3, and rips plants compared with wild type (WT) and osfh5 plants. Bar = 10 cm. (d) Height of mature WT, osfh5, and rips plants. n=15, ** P<0.01. (e) Phenotype of WT, osfh5, and rips seeds, showing defects in seed length and smoothness. Bar = 0.5cm.

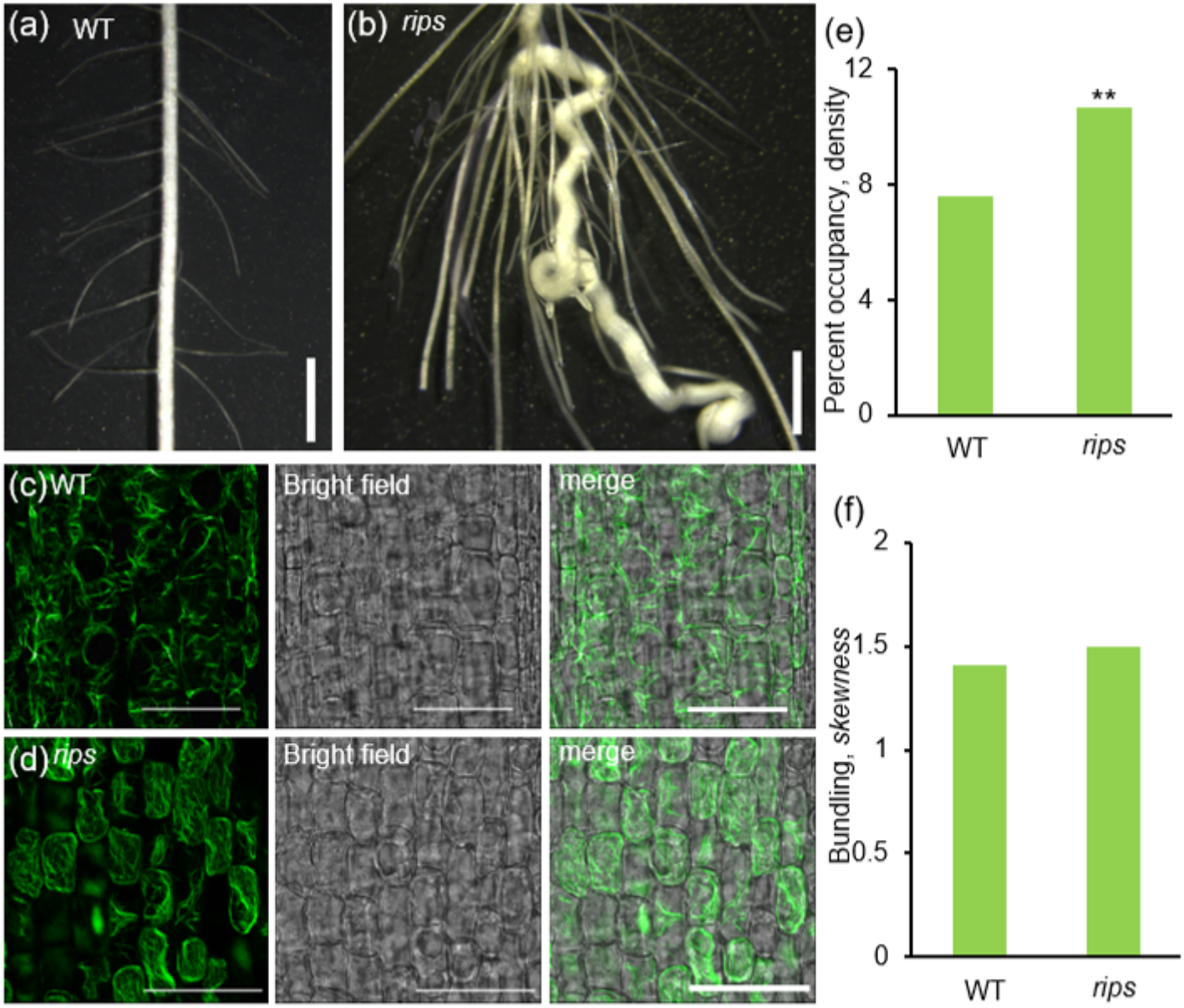

Figure 6

Rips knockout lines exhibited microfilament defects. (a, b) Roots of 5 days old wild type (WT) and rips plants in asana mirror. Bar = 2mm. (c, d) Root tips microfilaments staining results of WT and rips. Bar=50μm. (e) Actin filament abundance, or percentage of occupancy, in WT and rips root tips. n = 40, ** P<0.005. (f) Actin filament bundling, or skewness, in WT and rips root tips. n = 40.

Supplementary Files

This is a list of supplementary files associated with this preprint. Click to download.

- SupplementalTableS1.xlsx
- SupplementalMaterials.docx